Available online at www.sciencedirect.com

SCIENCE DIRECT®

Journal of Solid State Chemistry 178 (2005) 2922–2926

JOURNAL OF SOLID STATE CHEMISTRY

www.elsevier.com/locate/jssc

Molten salt flux synthesis and structure of the new layered uranyl tellurite, $K_4[(UO_2)_5(TeO_3)_2O_5]$

Jonathan D. Woodward, Thomas E. Albrecht-Schmitt*

Department of Chemistry and Biochemistry, E.C. Leach Nuclear Science Center, Auburn University, Auburn, AL 36849, USA

Received 26 May 2005; received in revised form 20 June 2005; accepted 28 June 2005

Abstract

The reaction of UO_3 and TeO_3 with a KCl flux at 800 °C for 3 days yields single crystals of $K_4[(UO_2)_5(TeO_3)_2O_5]$. The structure of the title compound consists of layered, two-dimensional ${}^{2}_{\infty}[(UO_2)_5(TeO_3)_2O_5]^{4-}$ sheets arranged in a stair-like topology separated by potassium cations. Contained within these sheets are one-dimensional uranium oxide ribbons consisting of UO_7 pentagonal bipyramids and UO_6 tetragonal bipyramids. The ribbons are in turn linked by corner-sharing with trigonal pyramidal TeO_3 units to form sheets. The lone-pair of electrons from the TeO_3 groups are oriented in opposite directions with respect to one another on each side of the sheets rendering each individual sheet nonpolar. The potassium cations form contacts with nearby tellurite units and axial uranyl oxygen atoms. Crystallographic data (193 K, Mo*K*α, $\lambda = 0.71073$ Å): triclinic, space group $P\bar{1}$, $a = 6.8514(5)$ Å, $b = 7.1064(5)$ Å, $c = 11.3135(8)$ Å, $\alpha = 99.642(1)°$, $\beta = 93.591(1)°$, $\gamma = 100.506(1)°$, $V = 531.48(7)$ Å^3, $Z = 1$, $R(F) = 4.19\%$ for 149 parameters and 2583 reflections with $I > 2\sigma(I)$.

Keywords: Layered structure; Uranyl compound; Uranyl tellurite; Stereochemically active lone-pair of electrons

1. Introduction

The uranyl tellurite system is remarkably rich and was first known from a few rare minerals including cliffordite, $UO_2(Te_3O_7)$ [1], moctezumite, $PbUO_2(TeO_3)_2$ [2], and schmitterite, $UO_2(TeO_3)$ [3]. The application of hydrothermal synthetic methods has resulted in a substantial expansion of this group to include $Pb_2UO_2(TeO_3)_3$ [4], $K[UO_2Te_2O_5(OH)]$ [5], $Tl_3\{(UO_2)_2[Te_2O_5(OH)](Te_2O_6)\} \cdot 2H_2O$ [5], α-$Tl_2[UO_2(TeO_3)_2]$ [6], β-$Tl_2[UO_2(TeO_3)_2]$ [5], $Sr_3[UO_2(TeO_3)_2(TeO_3)_2]$ [5], and $Na_8[(UO_2)_6(TeO_3)_{10}]$ [6]. Most recently we have shown that unlike iodates, mild hydrothermal conditions are not required from a thermodynamic standpoint to synthesize these compounds, and that relatively high-temperature molten salts can be used to facilitate the crystal growth of novel uranyl tellurites as demonstrated in our report on $A_2[(UO_2)_3(TeO_3)_2O_2]$ (A = K, Rb, and Cs) [7].

Continued interest in the uranyl tellurite system stems from the fact that these compounds defy normal topological trends in uranium oxides. The expectation is that extended structures containing uranyl cations will be layered, and contain U(VI) in the form of a UO_7 pentagonal bipyramid with an approximately linear UO_2^{2+}, uranyl, core [8]. However this is simply not the case in this system. For example, $K[UO_2Te_2O_5(OH)]$, β-$Tl_2[UO_2(TeO_3)_2]$ and $Sr_3[UO_2(TeO_3)_2(TeO_3)_2]$ contain UO_6 tetragonal bipyramids [5,6]; while $UO_2(Te_3O_7)$ incorporates UO_8 hexagonal bipyramids [1]. $PbUO_2(TeO_3)_2$, $UO_2(TeO_3)$, $Pb_2UO_2(TeO_3)_3$, α-$Tl_2[(UO_2)(TeO_3)_2]$, $Na_8[(UO_2)_6(TeO_3)_{10}]$, and Tl_3 $\{(UO_2)_2[Te_2O_5(OH)](Te_2O_6)\} \cdot 2H_2O$ all contain the more common UO_7 pentagonal bipyramid. It is also possible for multiple U(VI)-containing polyhedra to be present as was found for

---

*Corresponding author. Department of Chemistry, 179 Chemistry Building, Auburn University, AL 36849, USA.
Fax: +1 (334) 844 6959.
E-mail address: albreth@auburn.edu (T.E. Albrecht-Schmitt).

0022-4596/$ - see front matter © 2005 Elsevier Inc. All rights reserved.
doi:10.1016/j.jssc.2005.06.043

$A_2[(UO_2)_3(TeO_3)_2O_2]$ ($A = $ K, Rb, and Cs), which possess both UO_6 tetragonal bipyramids and UO_7 pentagonal bipyramids [7].

This system is made even more intricate by examining the coordination environment around the Te(IV) centers. $PbUO_2(TeO_3)_2$ [2], $Pb_2UO_2(TeO_3)_3$ [4], β-$Tl_2[UO_2(TeO_3)_2]$ [5], $Sr_3[UO_2(TeO_3)_2(TeO_3)_2]$ [5], $Na_8[(UO_2)_6(TeO_3)_{10}]$ [6], and $A_2[(UO_2)_3(TeO_3)_2(O)_2]$ ($A = $ K, Rb, and Cs) [7] all possess approximately C_{3v} tellurite, TeO_3, units. Whereas $UO_2(TeO_3)$ [3], $K[UO_2Te_2O_5(OH)]$ [5], and $Tl_3\{(UO_2)_2[Te_2O_5(OH)](Te_2O_6)\} \cdot 2H_2O$ [5] contain one-dimensional chains of corner-sharing, square pyramidal TeO_4 units. Finally, TeO_5 moieties are found in $UO_2(Te_3O_7)$ [1]. The structure α-$Tl_2[(UO_2)(TeO_3)_2]$ is particularly interesting in that it contains both TeO_3 and the rarely observed Te_2O_6 group [6].

While there is a general tendency for uranyl compounds to adopt layered structures [8], there is a propensity for uranyl compounds containing a main group element with a stereochemically active lone-pair of electrons, e.g. Se(IV) and I(V), to adopt one-dimensional topologies, although there are many exceptions to this [9–23]. This might be because the lone-pair of electrons blocks one dimension of propagation. True to the other oddities of uranyl tellurites, they do not follow expected dimensionality trends for either simple uranyl compounds, or for those with oxoanions containing a lone-pair of electrons. $PbUO_2(TeO_3)_2$ [2], β-$Tl_2[UO_2(TeO_3)_2$ [5], and $Sr_3[UO_2(TeO_3)_2(TeO_3)_2]$ [5] are one-dimensional, $UO_2(TeO_3)$ [3], α-$Tl_2[UO_2(TeO_3)_2]$ [6], $K[UO_2Te_2O_5(OH)]$ [5], $Tl_3\{(UO_2)_2[Te_2O_5(OH)](Te_2O_6)\} \cdot 2H_2O$ [5], and $A_2[(UO_2)_3(TeO_3)_2O_2]$ ($A = $ K, Rb, and Cs) [7] are two-dimensional, and $UO_2(Te_3O_7)$ [1], $Pb_2UO_2(TeO_3)_3$ [4], and $Na_8[(UO_2)_6(TeO_3)_{10}]$ [6] have three-dimensional network structures. Clearly not enough information is known about uranyl tellurites to establish any structural trends. In this paper we further expand the uranyl tellurite system through the application of a molten salt route that yields single crystals of a new potassium uranyl tellurite, $K_4[(UO_2)_5(TeO_3)_2O_5]$.

2. Experimental

Syntheses. UO_3 (99.8%, Strem), TeO_3 (99.9%, CERAC), and KCl (99.9%, Fisher) were used as received. SEM/EDX analyses were performed using a JEOL 840/Link Isis instrument. K, U, and Te percentages were calibrated against standards. *Caution! While UO_3 contains depleted U, standard procedures for handling radioactive material should be followed.*

$K_4[(UO_2)_5(TeO_3)_2O_5]$. The reactants UO_3 (177 mg, 0.620 mmol), TeO_3 (73 mg, 0.413 mmol), and KCl (250 mg, 3.35 mmol) were loaded into fused alumina crucible. The crucibles were heated in a box furnace at 800 °C for 3 days. The heating rate was 5 °C/min and the cooling rate was 0.50 °C/min. The resultant mixture in the crucible consisted of well-formed yellow prisms of $K_4[(UO_2)_5(TeO_3)_2O_5]$ as well as poorly formed orange crystals of an undefined product.

2.1. Crystallographic studies

A yellow prism of $K_4[(UO_2)_5(TeO_3)_2O_5]$ ($0.030 \times 0.043 \times 0.165\,mm^3$) suitable for single crystal X-ray diffraction experiments was selected using a stereomicroscope and mounted on a thin glass fiber with epoxy. The mounted crystal was secured on a goniometer head, cooled to −80 °C with an Oxford Cryostat, and optically aligned on a Bruker SMART APEX CCD X-ray diffractometer using a digital camera. A rotation photo was taken, and a preliminary unit cell was determined from three sets of 30 frames with 10 s exposure times using SMART software. All intensity measurements were performed using a graphite monochromator utilizing Mo$K\alpha$ radiation ($\lambda = 0.71073$ Å) from a sealed tube with a monocapillary collimator. The intensities of reflections of a sphere were collected by a combination of 3 sets of exposures. Each set had a different ϕ angle for the crystal, and each exposure covered a range of 0.3° in ω. A total of 1800 frames were collected with an exposure time per frame of 30 s.

Determination of integrated intensities and global cell refinement were performed with the Bruker SAINT (v. 6.02) software package using a narrow-frame integration algorithm. A face-indexed numerical absorption correction was initially applied using XPREP [24]. Individual shells of unmerged data were corrected analytically and exported in the same format. These files were subsequently treated with a semi-empirical absorption correction by SADABS [25]. The program suite SHELXTL (v 5.1) was used for space group determination (XPREP), direct methods structure solution (XS), and least-squares refinement (XL) [24]. The final refinement included anisotropic displacement parameters for all atoms and a secondary extinction parameter. Crystallographic details are listed in Table 1, atomic coordinates and isotropic thermal parameters are provided in Table 2, and selected bond lengths and angles are available in Table 3. Additional details can be found in Supporting Information.

3. Results and discussion

3.1. Structure of $K_4[(UO_2)_5(TeO_3)_2(O)_5]$

The structure $K_4[(UO_2)_5(TeO_3)_2O_5]$ consists of layered, two-dimensional ${}^2_\infty[(UO_2)_5(TeO_3)_2O_5]^{4-}$ sheets extending in the [*bc*] plane separated by K^+ cations. The sheets are comprised of uranyl oxide chains connected by corner-sharing, trigonal pyramidal TeO_3^{2-} ligands.

Table 1
Crystallographic data for $K_4[(UO_2)_5(TeO_3)_2O_5]$

Formula	$K_4[(UO_2)_5(TeO_3)_2O_5]$
Formula mass (amu)	1937.75
Color and habit	Yellow prism
Crystal system	Triclinic
Space group	$P\bar{1}$
a (Å)	6.8514(5)
b (Å)	7.1064(5)
c (Å)	11.3135(8)
= (deg.)	99.642(1)
β (deg.)	93.591(1)
γ (deg.)	100.506(1)
T (°C)	–80
V (Å^3)	531.48(7)
Z	1
λ (Å)	0.71073
Maximum 2θ (deg.)	56.60
ρ_{calcd} (g cm^{-3})	6.054
μ(Mo$K\alpha$) (cm^{-1})	415.26
$R(F)$ for $F_o^2 > 2\sigma(F_o^2)$[a]	0.0419
$R_w(F_o^2)$[b]	0.1313

[a] $R(F) = \sum ||F_o| - |F_c|| / \sum |F_o|$.
[b] $R_w(F_o^2) = [\sum[w(F_o^2 - F_c^2)^2] / \sum wF_o^4]^{1/2}$.

Table 2
Atomic coordinates and equivalent isotropic displacement parameters for $K_4[(UO_2)_5(TeO_3)_2O_5]$

Atom	x	y	z	U_{eq} (Å^2)[a]
U(1)	0.1242(1)	0.5686(1)	0.1805(1)	0.011(1)
U(2)	0	0	0	0.011(1)
U(3)	0.2231(1)	0.1234(1)	0.3156(1)	0.012(1)
Te(1)	0.6825(1)	0.3196(1)	0.5147(1)	0.013(1)
K(1)	0.5627(3)	0.2947(3)	0.0830(2)	0.022(1)
K(2)	0.3036(3)	0.1630(3)	0.7327(2)	0.020(1)
O(1)	0.3799(12)	0.6189(11)	0.1327(8)	0.021(2)
O(2)	−0.1228(13)	0.5212(11)	0.2376(9)	0.023(2)
O(3)	0.0817(10)	0.8734(9)	0.1635(7)	0.014(1)
O(4)	0	$\frac{1}{2}$	0	0.039(3)
O(5)	0.1306(10)	0.2466(9)	0.1517(7)	0.014(1)
O(6)	0.2542(12)	0.0091(12)	−0.0490(7)	0.019(2)
O(7)	0.4708(11)	0.1220(11)	0.2643(7)	0.017(2)
O(8)	−0.0146(12)	0.1266(11)	0.3787(8)	0.022(2)
O(9)	0.4080(11)	0.2288(11)	0.5089(7)	0.020(2)
O(10)	0.7098(12)	0.5292(10)	0.6427(7)	0.022(2)
O(11)	0.7631(12)	0.1771(10)	0.6264(7)	0.021(2)

[a] U_{eq} is defined as one-third of the trace of the orthogonalized $\boldsymbol{U}_{ij}$ tensor.

Table 3
Selected bond distances (Å) for $K_4[(UO_2)_5(TeO_3)_2O_5]$

U(1)–O(2)	1.843(8)	U(2)–O(3)′	2.271(7)
U(1)–O(1)	1.856(8)	U(2)–O(6)′	1.854(8)
U(1)–O(4)	2.1048(4)	U(3)–O(8)	1.820(8)
U(1)–O(5)	2.266(6)	U(3)–O(7)	1.829(7)
U(1)–O(3)	2.274(6)	U(3)–O(3)′	2.280(7)
U(1)–O(10)′	2.499(7)	U(3)–O(5)	2.282(7)
U(1)–O(11)′	2.567(8)	U(3)–O(11)′	2.352(6)
U(1)–O(2)	1.843(8)	U(3)–O(10)′	2.387(7)
U(1)–O(1)	1.856(8)	U(3)–O(9)	2.388(8)
U(2)–O(6)′	1.854(8)	U(3)–O(8)	1.820(8)
U(2)–O(6)	1.854(8)	Te(1)–O(11)	1.864(7)
U(2)–O(5)′	2.246(7)	Te(1)–O(9)	1.867(7)
U(2)–O(5)	2.246(7)	Te(1)–O(10)	1.869(7)
U(2)–O(3)′	2.271(7)		

The chains, extending along the b axis, are composed of pentagonal bipyramidal UO_7 and tetragonal bipyramidal UO_6 moieties. Oxygen atoms from TeO_3 moieties and bridging oxo ligands coordinate each of the uranyl units equatorially. The chains consist of corner-sharing pentagonal bipyramidal UO_7 dimers edge-shared to trimers consisting of UO_7 pentagonal bipyramids edge-shared with intermediary UO_6 tetragonal bipyramids. The bridging TeO_3 units join the UO_7 units of both the dimers and trimers on adjacent chains and simultaneously form the edges and two opposite corners of UO_7 pentagonal bipyramids. The coordination polyhedra of the uranium atoms are completed by μ_2-O^{2-} ligands that bridge the UO_7 dimers and μ_3-O^{2-} ligands that are shared by both the UO_7 moieties and the intermediary UO_6 tetragonal bipyramids. Thus, each UO_7 unit from the dimer forms three U–O bonds with the oxo ligands and two bonds with the TeO_3^{2-} anions. In contrast, the peripheral UO_7 units from the trimer each form two U–O bonds with the oxo ligands and three bonds with the tellurite groups while the UO_6 moieties each form four U–O bonds with the oxo ligands. The chains of tellurite ligands have their stereochemically active lone-pair of electrons oriented in opposite directions with respect to one another on each side of the sheet, rendering the individual sheets non-polar. The basic building unit of $K_4[(UO_2)_5(TeO_3)_2O_5]$, depicting the coordination environment of the uranium and tellurium atoms, is given in Fig. 1. A polyhedral representation of part of a single two-dimensional $^2_\infty[(UO_2)_5(TeO_3)_2O_5]^{4-}$ sheet is shown in Fig. 2.

The U$=$O bond lengths from the tetragonal bipyramidal UO_6 units are 1.854(8) Å. These bond lengths are similar to those in the pentagonal bipyramidal UO_7 moieties, which have U$=$O bond lengths of 1.856(8) Å and 1.843(8) Å for U(1) and 1.820(8) Å and 1.829(7) Å for U(3). It is noteworthy that the uranyl bonds in this compound are slightly longer than expected. This has been observed before in other uranyl compounds with oxoanions containing a lone-pair of electrons [5]. The equatorial bond lengths in the pentagonal bipyramidal UO_7 units show significant variations of the U–O distances, ranging from 2.1048(4) Å to 2.567(8) Å for U(1) and 2.280(7) Å to 2.388(8) Å for U(3). The UO_6 groups are also distorted with equatorial bond lengths of 2.271(7) Å ($\times 2$) and 2.246(7) Å ($\times 2$). These distortions are due to differences in the coordination

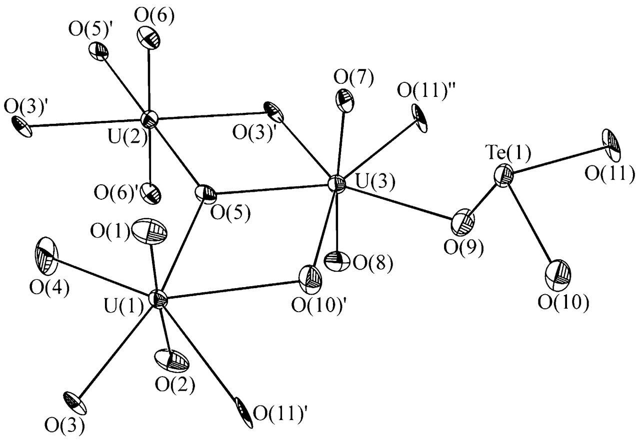

Fig. 1. A view of the fundamental building units in $K_4[(UO_2)_5(TeO_3)_2O_5]$ consisting of two crystallographically unique pentagonal bipyramidal UO_7 units, a tetragonal bipyramidal UO_6 unit, and trigonal pyramidal TeO_3 groups. A 50% probability ellipsoids are shown.

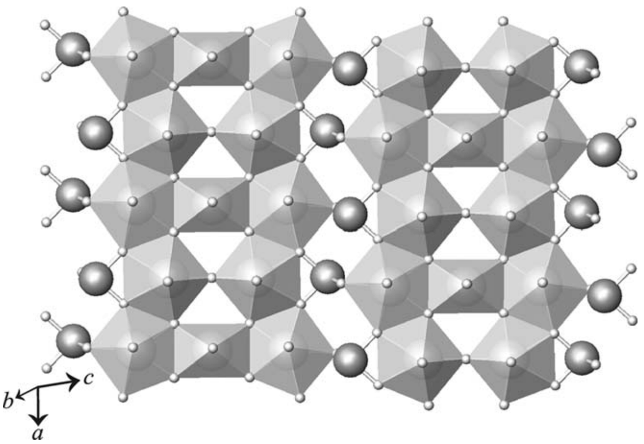

Fig. 2. An illustration of the $^2_\infty[(UO_2)_5(TeO_3)_2O_5]^{4-}$ sheets in $K_4[(UO_2)_5(TeO_3)_2O_5]$. The one-dimensional uranium oxide chains extending along the *b*-axis, shown in polyhedral form, consist of corner-sharing pentagonal bipyramidal UO_7 dimers edge-shared to trimers econsisting of UO_7 pentagonal bipyramids edge-shared with intermediary UO_6 tetragonal bipyramids. The chains are linked by corner-sharing trigonal pyramidal TeO_3 units, shown in ball-and-stick form, to form the sheets.

of the TeO_3 moieties to the uranyl units versus coordination by the μ_2-O^{2-} and μ_3-O^{2-} oxo anions. The U–O bonds from the tellurite oxygen atoms represent the long equatorial bonds while the μ_2-O and μ_3-O atoms produce the short U–O equatorial bonds.

The TeO_3 ligands deviate significantly from idealized C_{3v} symmetry, exhibiting Te–O bond length variations consistent with their bridging modes to the uranium centers. The shorter Te–O bonds are to the μ_2-O(9) and μ_3-O(11) atoms (1.866(7) Å and 1.864(7) Å) while the longer Te–O bonds are to the μ_3-O(10) atoms (1.869(7) Å). The Te–O bond lengths are similar to those found in other uranyl tellurites [1–7]. Bond valence sum calculations provide values of 5.88, 5.85, 5.91, and 4.05 for **1** for U(1), U(2), U(3), and Te(1), respectively. These bond valence sums support that this compound contains U(VI) and Te(IV) centers [26,27]. Parameters for six- and seven-coordinate U(VI) atoms from Burns et al. were used in this calculation [28].

The K^+ cations are found between the $^2_\infty[(UO_2)_5(TeO_3)_2O_5]^{4-}$ sheets. The cations interact with oxygen atoms from the UO_2^{2+} and TeO_3^{2-} anions between adjacent sheets. Depending on where one establishes the maximum length for $K^+ \cdots O$ contacts, there are between seven and eight interactions with $K^+ \cdots O$ distances ranging from 2.614(8) to 3.347(2) Å. The shortest separation between the Te(IV) centers and the K^+ cations is 3.837(2) Å. These distances are similar to those found in $K[UO_2Te_2O_5(OH)]$ [5]. Based on this long distance, there is no evidence for interactions between the lone-pair of electrons and the alkali metal cations; in fact, the lone-pairs are directed opposite to the cations. A view depicting the cation-separated sheets of $K_4[(UO_2)_5(TeO_3)_2O_5]$, within the [*ac*] plane, is shown in Fig. 3. The Te atoms are not coplanar with adjacent U atoms that comprise the uranium oxide one-dimensional chains, thus giving rise to stair-like topology of the sheets.

The structure of $K_4[(UO_2)_5(TeO_3)_2O_5]$ is similar to that observed in compounds with the guilleminite sheet topology, which is known for $Ba[(UO_2)_3(SeO_3)_2O_2] \cdot 3H_2O$ (guilleminite) [22], marthozite, $Cu[(UO_2)_3(SeO_3)_2O_2] \cdot 8H_2O$ [23], and $Sr[(UO_2)_3(SeO_3)_2O_2] \cdot 4H_2O$ [29]. Layers in these compounds are composed of chains of edge-sharing UO_7 pentagonal bipyramids and UO_8 hexagonal bipyramids that are bridged by SeO_3^{2-} anions. The linking of the uranium oxide substructure in these sheets by the selenite groups also yields a staircase structure as found for $K_4[(UO_2)_5(TeO_3)_2O_5]$. The structures of $A_6(UO_2)_5(VO_4)_2O_5$ (A = Na, K) [30] and α- and β-$Rb_6U_5V_2O_{23}$ [31] also contain the same kind of

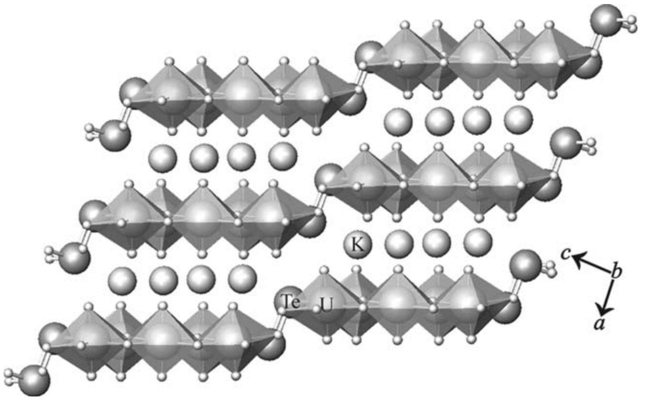

Fig. 3. A depiction of the structure of $K_4[(UO_2)_5(TeO_3)_2O_5]$ viewed perpendicular to the two-dimensional sheets along the *a*-axis showing the location of the interlayer K^+ cations.

uranium oxide ribbon as found in $K_4[(UO_2)_5(TeO_3)_2O_5]$, but these are instead linked by vanadate tetrahedra. There are also four uranyl compounds that contain sheets of edge-sharing $[UO_7]$ units linked by $[UO_6]$ polyhedra similar to the uranium oxide ribbons in $K_4[(UO_2)_5(TeO_3)_2O_5]$. These compounds include β-U_3O_8 [32], Wyartite, $CaU(UO_2)_2(CO_3)O_4(OH)(H_2O)_7$ [33], Ianthinite, $[U_2(UO_2)_4O_6(OH)_4(H_2O)_4](H_2O)_5$ [34], and Spriggite, $Pb_3[(UO_2)_6O_8(OH)_2](H_2O)_3$ [35]. The sheets in $K_4[(UO_2)_5(TeO_3)_2O_5]$ can be viewed as containing ribbons that have been excised from the sheet topology of these compounds that are linked by TeO_3 units.

4. Conclusions

The recent massive expansion of uranyl-containing inorganic compounds from 180 in 1996 to over 350 in 2005 might lead one to speculate that most new structure types have been discovered, particularly for those with two-dimensional topologies. The successful preparation of the novel layered alkali metal uranyl tellurite, $K_4[(UO_2)_5(TeO_3)_2O_5]$, together with many other recent examples, demonstrates that this is far from the case, and that there is likely much more to be discovered. This goal will be realized by the application of hydrothermal methods, molten salt fluxes, high-temperature solid-state syntheses, and room-temperature crystallization.

Auxiliary Material: Further details of the crystal structure investigation may be obtained from the Fachinformationzentrum Karlsruhe, D-76344 Eggenstein-Leopoldshafen, Germany (Fax: (+49)7247-808-666; Email: crysdata@fiz-karlsruhe.de) on quoting depository numbers CSD 415463.

Acknowledgment

This work was supported by the Department of Energy, Office of Basic Energy Sciences, Heavy Elements Program (Grant No. DE-FG02-01ER15187).

References

[1] (a) J. Galy, G. Meunier, Acta Crystallogr. B 27 (1971) 608;
    (b) F. Branstätter, Tschermaks Mineral. Petrogr. Mitt. 29 (1981) 1.
[2] G.H. Swihart, P.K.S. Gupta, E.O. Schlemper, M.E. Back, R.V. Gaines, Am. Mineral. 78 (1993) 835.
[3] G. Meunier, J. Galy, Acta Crystallogr. B 29 (1973) 1251.
[4] F. Branstätter, Z. Kristallogr. 155 (1981) 193.
[5] P.M. Almond, M.L. McKee, T.E. Albrecht-Schmitt, Angew. Chem. Int. Ed. 41 (2002) 3426.
[6] P.M. Almond, T.E. Albrecht-Schmitt, Inorg. Chem. 41 (2002) 5495.
[7] J.D. Woodward, P.M. Almond, T.E. Albrecht-Schmitt, J. Solid State Chem. 177 (2004) 3971.
[8] (a) P.C. Burns, M.L. Miller, R.C. Ewing, Can. Mineral. 34 (1996) 845;
    (b) P.C. Burns, in: P.C. Burns, R. Finch (Eds.), Uranium: Mineralogy, Geochemistry and the Environment, Mineralogical Society of America, Washington, DC, 1999 (Chapter 1);
    (c) P.C. Burns, Mater. Res. Soc. Symp. Proc. 802 (2004) 89.
[9] R.E. Sykora, D.M. Wells, T.E. Albrecht-Schmitt, Inorg. Chem. 41 (2001) 2304.
[10] A.C. Bean, S.M. Peper, T.E. Albrecht-Schmitt, Chem. Mater. 13 (2001) 1266.
[11] A.C. Bean, M. Ruf, T.E. Albrecht-Schmitt, Inorg. Chem. 40 (2001) 3959.
[12] A.C. Bean, C.F. Campana, O. Kwon, T.E. Albrecht-Schmitt, J. Am. Chem. Soc. 123 (2001) 8806.
[13] A.C. Bean, T.E. Albrecht-Schmitt, J. Solid State Chem. 161 (2001) 416.
[14] P.M. Almond, S.M. Peper, E. Bakker, T.E. Albrecht-Schmitt, J. Solid State Chem. 168 (2002) 358.
[15] P.M. Almond, T.E. Albrecht-Schmitt, Inorg. Chem. 41 (2002) 1177.
[16] B.O. Loopstra, N.P. Brandenburg, Acta Crystallogr. B 34 (1978) 1335.
[17] V.E. Mistryukov, Y.N. Michailov, Koord. Khim. 9 (1983) 97.
[18] D. Ginderow, F. Cesbron, Acta Crystallogr. C 39 (1983) 824.
[19] D. Ginderow, F. Cesbron, Acta Crystallogr. C 39 (1983) 1605.
[20] M. Koskenlinna, J. Valkonen, Acta Crystallogr. C 52 (1996) 1857.
[21] M. Koskenlinna, I. Mutikainen, T. Leskelae, M. Leskela, Acta Chem. Scand. 51 (1997) 264.
[22] M.A. Cooper, F.C. Hawthorne, Can. Mineral. 33 (1995) 1103.
[23] M.A. Cooper, F.C. Hawthorne, Can. Mineral. 39 (2001) 797.
[24] G.M. Sheldrick, SHELXTL PC, Version 6.12, An Integrated System for Solving, Refining, and Displaying Crystal Structures from Diffraction Data, Siemens Analytical X-ray Instruments, Inc., Madison, WI, 2001.
[25] G.M. Sheldrick, *SADABS* 2001, Program for absorption correction using SMART CCD based on the method of Blessing: R.H. Blessing, Acta Crystallogr. A 51 (1995) 33.
[26] I.D. Brown, D. Altermatt, Acta Crystallogr. B 41 (1985) 244.
[27] N.E. Brese, M. O'Keeffe, Acta Crystallogr. B 47 (1991) 192.
[28] P.C. Burns, R.C. Ewing, F.C. Hawthorne, Can. Mineral. 35 (1997) 1551.
[29] P.M. Almond, T.E. Albrecht-Schmitt, Am. Mineral. 89 (2004) 976.
[30] C. Dion, S. Obbade, E. Raekelboom, F. Abraham, M. Saadi, J. Solid State Chem. 155 (2000) 342.
[31] S. Obbade, C. Dion, L. Duvieubourg, M. Saadi, F. Abraham, J. Solid State Chem. 173 (2003) 1.
[32] B.O. Loopstra, Acta Crystallogr. B 26 (1970) 656.
[33] P.C. Burns, R.J. Finch, Am. Mineral. 84 (1999) 1456.
[34] P.C. Burns, F.C. Hawthorne, M.L. Miller, R.C. Ewing, J. Nucl. Mater. 249 (1997) 199.
[35] J. Brugger, S.V. Krivovichev, P. Berlepsch, N. Meisser, S. Ansermet, T. Armbruster, Am. Mineral. 89 (2004) 339.